cm^{-3}) and the insensitivity of its electronic and electrochemical properties to annealing in O_2 has been demonstrated.[10]

Since the flow of charge from one material to the other, to achieve electronic equilibrium, is dependent upon the relative positions of the Fermi levels before contact, there is considerable question as to direction and extent of "band bending" at the VOPc/PTCDA or CuPc/PTCDA interface. Because of the low charge densities believed prevalent in PTCDA thin films, there is even some question whether electronic equilibrium is achieved with these systems in the dark. Forrest and co-workers have argued, for the CuPc/PTCDA system, that a p-p′ isotype heterojunction is formed[8] and the band diagrams they used to describe the CuPc/PTCDA system would produce the type of rectification observed in our studies. Nevertheless, there is some disagreement in their positioning of the "band edges" for the CuPc and the PTCDA versus those of VOPc and PTCDA we show here, which would introduce different band discontinuities at the interface between the two materials.

Previous studies of photovoltaics produced from phthalocyanine/perylene bilayers have all suggested that the junction properties of these systems were determined by a narrow region of material near the Pc/Pe interface and that the junction potentials are dependent to some extent on the relative ionization potentials and electron affinities of the two contacting phases.[1,2,8] The studies shown here suggest that photocurrent arises principally from a region quite near the VOPc/PTCDA interface, which is consistent with a sharp change in electric field gradient at that interface, assisting exciton dissociation. In this sense the VOPc/PTCDA interface may act like a fixed site impurity, as proposed by Popovic,[12] to provide a large local electric field to assist in exciton dissociation. The fact that the transient photocurrent increased in relation to the total number of VOPc/PTCDA interfaces is consistent with a simple increase in the number of such exciton dissociation sites. Excitons created well away from these interfaces are less likely to contribute to photocurrent generation, unless bulk dissociation, at other structural or chemical impurity sites, is significant. It is interesting to note that some organization of the Pc and PTCDA as thin films is necessary in order to realize the full effect of the VOPc/PTCDA interface—codeposited films do not suffice. Experiments are underway to create highly organized Pc/Pe interfaces, by a molecular beam epitaxy process, which will allow for extension of the studies reported here to much thinner films, as is reported in this journal for other phthalocyanine systems.[28]

Registry No. VOPc, 13930-88-6; CuPc, 147-14-8; PTCDA, 128-69-8; Au, 7440-57-5; hydroquinone, 123-31-9; anthraquinone sulfonate, 30637-95-7.

---

(28) (a) Nebesny, K. W.; Collins, G. E.; Lee, P. A.; Chau, L.-K.; Danziger, J.; Osburn, E.; Armstrong, N. R. *Chem. Mater.* Following article in this issue. (b) Armstrong, N. R.; Nebesny, K. W.; Collins, G. E.; Lee, P. A.; Chau, L.-K.; Arbour, C.; Parkinson, B. A.; Proceedings, SPIE Symposium 1559, *Photopolymer Device Physics and Applications*; in press.

Organic/Inorganic Molecular Beam Epitaxy: Formation of an Ordered Phthalocyanine/SnS_2 Heterojunction

K. W. Nebesny,* G. E. Collins, P. A. Lee, L.-K. Chau, J. Danziger, E. Osburn, and N. R. Armstrong*

Department of Chemistry, University of Arizona, Tucson, Arizona 85721

Received April 9, 1991

We report the growth of thin films of the metal dichalcogenide, SnS_2, on cleaved mica surfaces, followed by the deposition of monolayers and multilayers of chloroindium phthalocyanine, InPc–Cl. Reflection high-energy electron diffraction (RHEED) was used to show that the SnS_2 thin films grew with a principal axis oriented along a principal axis of the mica substrate, even at submonolayer coverages of SnS_2. X-ray photoelectron spectroscopy (XPS), reflection electron energy loss spectroscopies (REELS), and optical spectroscopies were used to confirm that the stoichiometry and electronic properties of these SnS_2 thin films were those of 2H-SnS_2. As with the deposition of InPc–Cl on melt-grown, bulk SnS_2, the first monolayer of InPc–Cl on SnS_2/mica gave RHEED patterns consistent with the formation of a closest packed monolayer, with the Pc's lying flat on the surface. On the MBE-grown SnS_2, InPc–Cl multilayer films were grown that gave the same RHEED patterns as seen for the monolayer deposits. These diffraction data are consistent with the buildup of each Pc monolayer in registry with the initial monolayer. Transmission optical spectra of these Pc thin films show a strong, narrow absorption spectrum, in sharp contrast to those seen for polycrystalline InPc–Cl deposits, suggesting that the Pc chromophores sit in essentially equivalent environments.

Introduction

The growth of thin film heterostructures via molecular beam epitaxy is a mature technology, allowing tailoring of physical and chemical properties of materials through the formation of single-layer and multilayer thin films, ordered at the atomic level, with z-axis dimensions that vary from atomic diameters to hundreds of angstroms for each layer.[1] In the preparation of most single-crystal thin films there is the general requirement that substrates and overlayers be chosen with commensurate or nearly commensurate

---

* To whom correspondence should be addressed.

(1) Bauer, E. G.; Dodson, B. W.; Ehrlich, D. J.; Feldman, L. J.; Flynn, P. C.; Geis, M. W.; Harbison, J. P.; Matyi, R. J.; Peercy, P. S.; Petroff, P. M.; Phillips, J. M.; Stringfellow, G. B.; Zangwill, A. *J. Mater. Res.* **1990**, *5*, 852.

structures in order to minimize lattice strain in the growing thin films.[2] It has recently been demonstrated, however, that it may be possible to grow a wide range of highly ordered heterojunction materials, both inorganic/inorganic′ and organic/inorganic, where both the substrate and the overlayer have significant lattice mismatch (≥10%), and where the interaction of the growing thin film with the substrate is proposed to occur principally through van der Waals forces.[3] Several intriguing reports have recently shown that layered compounds, like the metal dichalcogenides (e.g., MoS_2, $MoSe_2$, SnS_2, $SnSe_2$, etc.), lend themselves to this type of single-crystal deposition, because of the lack of dangling bonds at the surfaces of these materials.[3,4] The layered transition-metal dichalcogenides have in common a metal cation in either a trigonal biprismatic (e.g., MoS_2) or octahedral (e.g., SnS_2) environment, with the cation completely surrounded by the chalcogenide atoms, and only weak forces binding the adjacent anion/cation/anion layers together.[4] Following the initial nucleation step, these layers grow readily over each other, or over substrates such as cleaved mica, producing interfaces that appear to be sharp over atomic dimensions.

We have an interest in extending the growth of such ordered thin films to include crystalline organic systems. Vacuum compatible, cyclic conjugated organic molecules, such as copper phthalocyanines (CuPc) or chloroindium phthalocyanine (InPc–Cl), can be deposited as single-crystal monolayers on surfaces such as MoS_2 and SnS_2.[5a,6] Koma and co-workers have recently reported on the epitaxial deposition of VOPc on single-crystal KBr and KCl surfaces.[5b] There are also reports of the growth of highly ordered layers of perylenes on amorphous substrates, which have a clear orientation only in the *z* direction.[5c,d] Even earlier studies suggested that ordered Pc's could be produced on specially heat-treated mica surfaces, although no optical characterization of these materials was conducted to confirm this.[5e] Weak forces appear to dominate in the formation of these single-crystal organic layers, allowing single-crystal growth without the need for the formation of a commensurate inorganic/organic interface. There would be clear advantages to the formation of multilayer single-crystal Pc thin films, both in the study of energy and electron transfer in such assemblies and in the development of new photoconductor materials and optical logic materials that complement existing inorganic systems.[7,8]

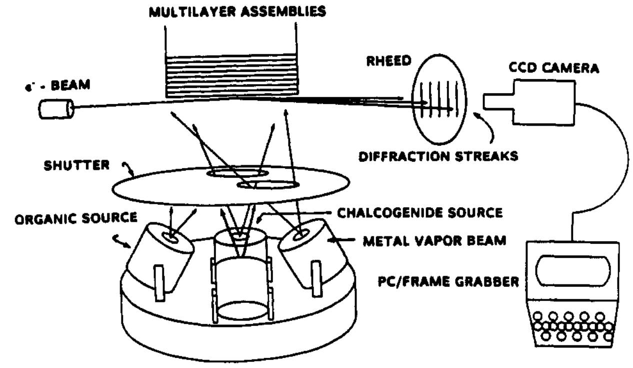

Figure 1. Schematic of the vacuum deposition system used to deposit SnS_2 on freshly cleaved mica and subsequently deposit InPc–Cl on SnS_2. The linear motion shutter, thickness monitors, and other leak sources not shown.

Our efforts have recently focused on the formation of new organic/inorganic (O/I) and organic/organic′ (O/O′) heterostructures and their optical, electrical, and photoelectrochemical characterization.[6,7] O/I structures have included phthalocyanine/metal and phthalocyanine/semiconductor assemblies, where the semiconductors include the above-mentioned metal dichalcogenides. SnS_2 has a bandgap energy E_{BG} = 2.2 eV, thus allowing illumination and optical characterization of epitaxially deposited dyes in the wavelength region beyond 550 nm.[6] In the case of deposition of submonolayer amounts of chloroindium phthalocyanine (InPc–Cl) on freshly cleaved, melt-grown SnS_2, it was found that these molecules could be deposited with a principal axis of the phthalocyanine oriented along one of the principle axes of the SnS_2 substrate (e.g., [11$\bar{2}$0]). When the resultant O/I heterostructure was immersed in electrolyte solutions, providing electrical contact to the SnS_2/InPc–Cl interface, illumination of the dye layer in the wavelength region 600–750 nm allowed for electron injection with a quantum efficiency per absorbed photon (QYAP) of nearly 50%. Under the growth conditions attempted to date, multilayer deposition of the Pc gave photocurrent yield spectra that indicated loss of the long-range ordering seen in the first monolayer. Beyond coverages of one monolayer the QYAP declined; however, at Pc coverages up to ca. 20–25 monolayers, the QYAP was sustained at ca. 20%. Recent preliminary scanning tunneling microscopic results suggest that multilayer deposits of InPc–Cl on highly ordered pyrolitic graphite may be ordered, over distances of ca. 20–50 molecular units.[7c]

We are presently pursuing more sophisticated heterojunction structures, especially those needed for study by transient optical spectroscopies and in the development of optical switching, by deposition of *both* the inorganic and organic thin films, through molecular beam epitaxy. It has been demonstrated that some of the metal dichalcogenides can be deposited epitaxially (using metal vapor beams and chalcogenide beams) on substrates with

---

(2) (a) Frank, F. C.; van der Merwe, J. H. *Proc. R. Soc.* London **1949**, *A198*, 216. (b) Kern, R.; Lelay, G.; Metois, J. J. In *Current Topics in Materials Science*; Kaldis, E., Ed.; North Holland: Amsterdam, 1979; p 130. (c) Vook, R. W. *Int. Met. Rev.* **1982**, *27*, 209.

(3) (a) Ohuchi, F. S.; Shimada, T.; Parkinson, B. A.; Ueno, K.; Koma, A. *J. Cryst. Growth*, in press. (b) Ohuchi, F. S.; Parkinson, B. A.; Ueno, K.; Koma, A. *J. Appl. Phys.* **1990**, *68*, 2168. (c) Ueno, K.; Koichiro, S.; Toshihiro, S.; Koma, A. *J. Vac. Sci. Technol.* **1990**, *A8*, 60. (d) Saiki, K.; Ueno, K.; Shimada, T.; Koma, A. *J. Cryst. Growth* **1989**, *95*, 603. (e) Koma, A.; Yoshimura, K. *Surf. Sci.* **1986**, *174*, 556.

(4) (a) Levy, F., Ed. *Crystallography and Crystal Chemistry of Materials with Layered Structures*; Reidel: Dordrecht, 1976. (b) Mooser, E., Ed. *Physics and Chemistry of Materials with Layered Structures*; Reidel: Dordrecht, 1976–79; Vols 1–6. (c) Doni, E.; Girlanda, R. In *Electronic Structure and Electronic Transitions in Layered Materials*; Grasso, V., Ed.; Reidel: Boston, 1986; pp 119–122. (d) Tributsch, H. *Struct. Bonding* **1982**, *49*, 127. (e) Palosz, B.; Steurer, W.; Schulz, H. *Acta Crystallogr.* **1990**, *B46*, 449.

(5) (a) Hara, M.; Sasabe, H.; Yamada, A.; Garito, A. F. *Jpn. J. Appl. Phys.* **1989**, *28*, L306. (b) Tada, H.; Saike, K.; Koma, A., *Jpn. J. Appl. Phys.* **1991**, *30*, L (c) Forrest, S. R.; Kaplan, M. L.; Schmidt, P. H. *Annu. Rev. Mater. Sci.* **1987**, *17*, 189. (d) Forrest, S. R.; Kaplan, M. L.; Schmidt, P. H. *J. Appl. Phys.* **1984**, *55*, 1492. (e) Uyeda, N.; Ashida, M.; Suito, E. *J. Appl. Phys.* **1965**, *36*, 1453.

(6) (a) Armstrong, N. R.; Nebesny, K. W.; Collins, G. E.; Lee, P. A.; Chau, L.-K.; Arbour, C.; Parkinson, B. A. In *Photopolymer Device Physics and Applications*; Lessard, R. A., Ed.; SPIE Symposium #1559; July, 1991, in press. (b) Armstrong, N. R., Nebesny, K. W.; Collins, G. E.; Chau, L.-K.; Lee, P. A.; England, C.; Diehl, D.; Danskey, M.; Parkinson, B. A. "Science and Technology of Thin Films for the 21st Century"; Chong, R. P. H., Ed.; *Thin Solid Films*, in press. (c) Arbour, C.; Nebesny, K. W.; Lee, P. A.; Chau, L.-K.; Armstrong, N. R.; Parkinson, B. A., manuscript in preparation.

(7) (a) Arbour, C.; Armstrong, N. R.; Brina, R.; Collins, G.; Danziger, J.; Dodelet, J.-P.; Lee, P. A.; Nebesny, K. W.; Pankow, J.; Waite, S. *Mol. Cryst. Liq. Cryst.* **1990**, *183*, 307. (b) Danziger, J.; Dodelet, J.-P.; Armstrong, N. R. *Chem. Mater.*, preceding article in this issue. (c) Nunnes, N.; Armstrong, N. R., unpublished results.

(8) Peyghambarian, N.; Koch, S. In *Nonlinear Photonics*; Gibbs, H., Khitrova, G., Peyghambarian, N., Eds.; Springer Series in Electronics and Photonics; Springer-Verlag: Berlin, 1990; Vol. 30, pp 7–60.

acceptable optical properties, such as freshly cleaved mica or CaF_2, with the achievement of excellent ordering in the first atomic layers.[3b] Lattice mismatch and incommensurate structures do not appear to be as problematic as might be expected, but the mechanism for formation of the single-crystal thin films of layered materials on such substrates is still not well understood and is the subject of intense study.

In this report we demonstrate the formation of SnS_2 thin films by epitaxial growth on mica substrates, using tin and sulfur vapor beams. Following the formation of the SnS_2 thin film, epitaxial deposition of monolayer *and* multilayers films of InPc–Cl is shown. The characterization of these layers by RHEED, XPS, REELS (reflection electron energy loss spectroscopy), and visible-wavelength spectroscopies suggests the formation of a unique form of Pc thin film, with a high degree of organization of the chromophore.

Experimental Section

Figure 1 shows a schematic of the combination of Knudsen cell sources used for these O/I-MBE experiments. These sources are all attached to a single ultrahigh vacuum flange, inserted into the base of a modified six-way cross deposition chamber, which is a simple extrapolation from previously described phthalocyanine deposition chambers from this group (base pressure ca. 10^{-10} Torr).[9] Each of these sources consists of a small boron nitride crucible (ca. 0.5–1.0-cm^3 internal volume) into which the powdered organic, metal sulfide or metal (Sn) is inserted. Each of these crucibles is inserted into a stainless steel body that contains several windings of tantulum wire, to provide the resistive heating necessary to bring these crucibles up to the appropriate deposition temperature. A separate thermocouple is attached to the base of each of the crucible heaters. Each Knudsen cell source and its associated thermocouple are attached to an Omega CN310 temperature controller, which provides the necessary heating (±0.5 °C) for creation of the metal, chalcogenide or Pc beams. The Knudsen cell producing the sulfur beam in these studies is more convenient to use than elemental sulfur, whose high vapor pressure and vacuum compatibility is problematic. We have found that purified iron pyrite (FeS_2), in powdered form (average particle diameter ca. 50 μm), when heated to ca. 550 °C at a base pressure of 10^{-10} Torr, produces a beam of sulfur which, from mass spectrometric analysis, appears to be principally diatomic sulfur. Precise control of sulfur flux was possible by using this source by simply controlling the source temperature to within ±10 °C. Further experiments are underway to explore the fluxes obtainable from such a source in the development of chalcogenide superlattices.[10]

Each of these Knudsen cell sources is isolated from the adjacent sources by metal fins, and the entire assembly is covered by a rotating shutter, which contains two openings to allow for simultaneous deposition of both metal and sulfur, or single-beam deposition of one or two different organic dyes. An additional shutter (not shown) on a linear motion feedthrough, was also used to separate this set of beam sources from the substrate upon which the SnS_2 and Pc were to be deposited. Experiments were conducted to confirm that there was no deposition of any of the materials from these beams when either shutter assembly was closed.

Thicknesses of the deposited films were determined by a quartz crystal thickness monitor (QCM, 10 MHz, ca. 4 Hz/ng cm^2), positioned in the center of the deposition chamber. The flux of metal was determined by using this QCM prior to the opening of the sulfur source. The sulfur flux was estimated by noting the increase in background pressure when this cell was opened to the deposition chamber. To ensure stoichiometric SnS_2 films, the rate of deposition of Sn was kept to ca. 2–10 Å/min, with the sulfur background pressure at 5×10^{-8} Torr. During phthalocyanine deposition the Pc flux was estimated by using the QCM, previously calibrated for deposition of such organics,[9] and from the time necessary to complete the first monolayer, as judged by the change in RHEED patterns (see below). The substrates, freshly cleaved mica samples (Precision Mica, V2 grade), were mounted on a modified x,y,z,360° manipulator that allowed for temperature control of the substrate during the SnS_2 and InPc–Cl depositions (see text).

The RHEED apparatus consisted of a 500-μm-diameter electron beam and associated 12-kV power supply and deflection electronics. The phosphor screen used was constructed from SnO_2-coated glass, and type 139 phosphor (Sylvania, Towanda, PA.). Diffraction streaks appearing on the phosphor screen were recorded photographically from the output of a CCD camera detector (Burle TC-65/EC Camera and Data Translation 2853 Frame Grabber). Postprocessing of the data was used to enhance the contrast in the diffraction streaks. Line scans have also been shown to aid in the interpretation. Beam currents were consistently kept below those that caused observable damage to the organic overlayers (made possible by the high sensitivity of the CCD camera).

X-ray photoelectron spectroscopy (XPS) and reflection electron energy loss spectroscopy (REELS) data were collected from a VG ESCALAB MKII spectrometer, with Al Kα radiation for the XPS studies. Data manipulation was conducted as described elsewhere,[11] so that for quantitation purposes, the inelastic background contributions to the spectra could be appropriately removed, and corrections made for photoionization cross section, escape depth, and instrument transmission functions. REELS spectra were obtained with the sample in the same position as for XPS. These spectra were occasionally used in the processing of the XPS data.[11]

Transmission optical spectra were obtained following deposition of the SnS_2 and the Pc in a dual beam spectrophotometer, with some correction made for the background absorbance of the mica substrate.

Results and Discussion

RHEED Results for SnS_2 Grown on Mica Substrates. The growth of highly ordered thin films of the metal dichalcogenides on freshly cleaved mica previously demonstrated for $MoSe_2$ and $NbSe_2$[3c] is confirmed for SnS_2 by the data below. Figure 2 shows the RHEED data for various coverages of SnS_2 on freshly cleaved mica and this same surface following deposition of various levels of InPc–Cl on the resultant SnS_2 layer. Figure 2a shows the RHEED pattern for a freshly cleaved mica surface, looking along the [100] azimuthal direction. The spacing between the principal diffraction lines is consistent with a lattice spacing of 5.19 Å. With the sulfur beam trained on the mica surface, with the Sn beam blocked from the surface by the shutter assembly, no changes in these diffraction patterns could be discerned, consistent with the notion that the chalcogenide atoms by themselves are not bound to the mica surface. Immediately upon introduction of the Sn beam to the deposition chamber (flux conditions described above), the diffraction lines of Figure 2a give way to those seen in Figure 2b, which represent the onset of growth of the SnS_2 lattice. At this point we estimate the coverage of SnS_2 to be ca. 0.5 ML (ML = monolayer), although this must be considered to be an average coverage and may represent patchwise formation of multilayer SnS_2 nuclei bordered by regions of bare mica. The new diffraction lines are present at a spacing consistent with a row-to-row spacing of sulfur of 3.15 Å.[4] It is significant that this ordering was observed without the need for reorientation of the underlying mica, suggesting that prin-

---

(9) Lee, P.; Pankow, J.; Danziger, J.; Nebesny, K. W.; Armstrong, N. R. In *Deposition and Growth, Frontiers for Microelectronics*; Rubeloff, G., Ed.; American Institute of Physics: New York, 1988; Vol. 167, pp 376–385.

(10) Nebesny, K. W.; Collins, G. A.; Lee, P. A.; Armstrong, N. R., manuscript in preparation.

(11) Nebesny, K. W.; Maschhoff, B. L.; Armstrong, N. R. *Anal. Chem.* 1989, *61*, 469A.

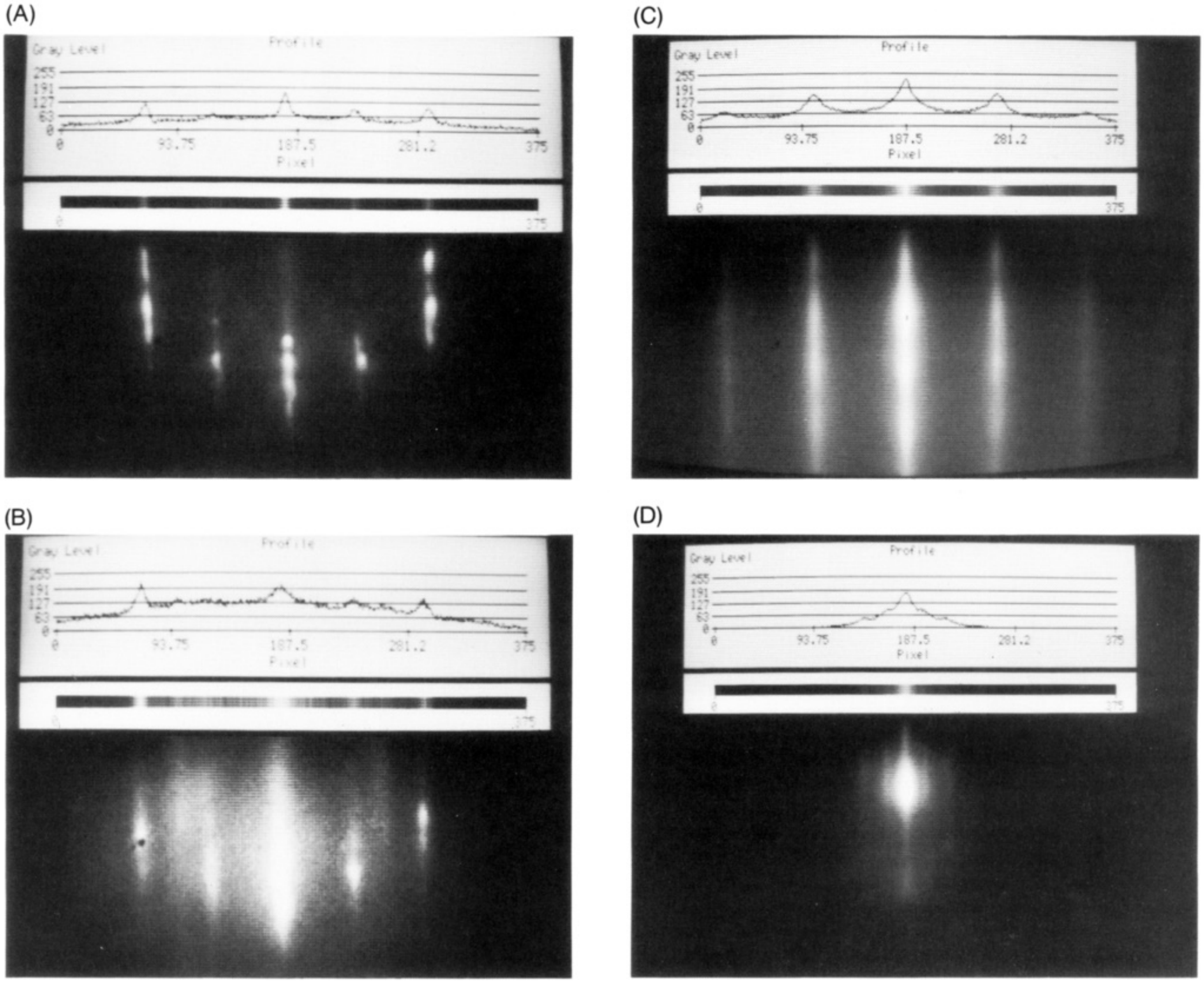

Figure 2. RHEED diffraction patterns obtained at various stages of thin film growth: (a) freshly cleaved mica, looking along the [100] direction, (b) after deposition of ca. 0.5 ML of SnS_2, (c) after completion of the first monolayer of SnS_2, and for all subsequent SnS_2 layers, looking along the [11$\bar{2}$0] direction, (d) diffraction pattern obtained after achieving 1 ML of InPc-Cl, and for all subsequent coverages of InPc-Cl, where the diffraction lines of (c) have been replaced with several closely spaced lines, achieved without the need to reorient the sample.

cipal axis [11$\bar{2}$0] of the SnS_2 overlayer is aligned along the [100] direction of the mica substrate. The expected SnS_2 pattern was obtained on a substrate for which the mismatch with the SnS_2 lattice is as much as ca. 65%. The possible mechanistic reasons for this are discussed further below. As with previous epitaxial deposition of similar dichalcogenides, rotation of the sample by 60° intervals at this stage reproduced these diffraction streaks and demonstrated the 6-fold symmetry of the SnS_2 film.[3]

Further deposition of SnS_2 on the mica substrate yields the RHEED pattern of Figure 2c. This diffraction pattern is typical of those seen for all coverages of SnS_2 on mica exceeding one monolayer. Rotation of the sample by 30° at this point gave rise to a diffraction pattern where less intense diffraction streaks are spaced at wider intervals, consistent with the smaller row-to-row sulfur spacing when looking at 30° rotation away from the [11$\bar{2}$0] axis[7] (see Figure 6). Previous RHEED studies of freshly cleaved bulk SnS_2 have yielded diffraction patterns similar to those shown in Figure 2c.[7] Continued deposition of tin and sulfur on this surface increases the SnS_2 thickness, as discussed below, but no further changes in the RHEED patterns are discerned, indicating that all subsequent SnS_2 layers are commensurate with the first layers deposited. With the sensitivity of the CCD camera technology to view the phosphor screen, another set of diffraction lines can be seen, with low intensity (ca. 30% of the intensity of the major diffraction lines spaced farthest away from the specular beam), which are spaced near those major lines seen in Figure 2c and are at the position of those seen for the 30° rotation. As the SnS_2/mica sample is rotated, these new lines intensify and then diminish in intensity. Such results have been noted for the deposition of other metal chalcogenides on mica before,[3c] and it has been suggested that this is due to "texturing" of the surface. A more reasonable explanation is that there is more than one domain of SnS_2 deposited on the mica surface, either as the result of different domains present in the mica substrate or because the growth mechanism permits the formation of a small percentage of the second SnS_2 domain oriented at ca. 30° with respect to the dominant SnS_2 domains. Recently experiments have shown that observation of these other SnS_2 domains is strongly dependent upon the quality of mica used in these studies (as judged by the number of visual imperfections and by the sharpness of the RHEED diffraction streaks). It is also possible to attenuate the presence of this extra domain of SnS_2, as judged by the extra RHEED streaks seen at the 30° ro-

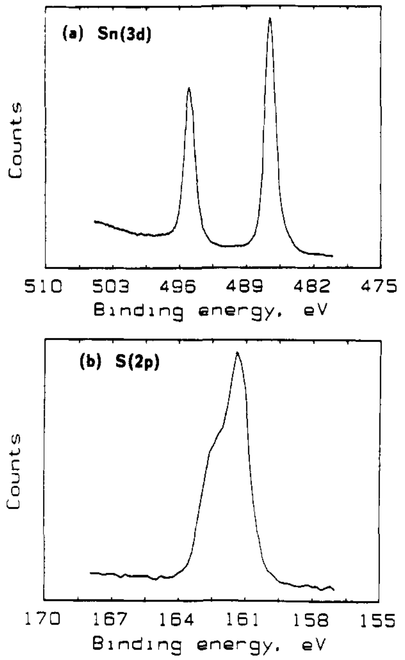

Figure 3. XPS spectra for SnS_2 deposited on freshly cleaved mica, representative of all coverages, including the submonolayer regime. The S(2p) spectrum was obtained at a high enough resolution to allow discrimination of the $S(2p_{1/2})$ and $S(2p_{3/2})$ transitions.

tation, through annealing of the SnS_2 film after growth (400 °C, 8 h).[10]

XPS/EELS Studies. SnS_2 Thin Films on Mica. Figure 3 shows XPS spectra typical of monolayer or multilayer coverages of SnS_2 on mica, with binding energies (BE) consistent with the formation of stoichiometric SnS_2 (BE for Sn(3d) = 487.1 eV, and BE for S(2p) = 162.1 eV, which leads to a $\Delta BE[Sn(3d_{5/2}) - S(2p_{3/2})] = 325.0$ eV, versus $\Delta BE = 324.8$ eV for freshly cleaved bulk SnS_2.[11] The stoichiometry of the SnS_2 film was confirmed by computing the relative atomic ratios, N_S/N_{Sn}, from Sn(3d) and S(2p) peak areas, for the thin films, and for bulk (melt grown) SnS_2, and comparing.[11] With the bulk SnS_2 as a standard, the thin films grown on mica showed $N_S/N_{Sn} = 2.04 \pm 0.05$. Similar spectra, with the same binding energy differences, and N_S/N_{Sn} ratios, were seen for *all* coverages of SnS_2 on the mica substrate, including the submonolayer coverage regime.

It was possible to produce substoichiometric films when the flux of sulfur was not sufficient to the surface. XPS data for some of these thin films showed N_S/N_{Sn} ratio as low as ca. 1.7, and a distinct splitting of the Sn(3d) and S(2p) peaks. In those cases, the new peaks were present at higher binding energies than those seen for the stoichiometric material by ca. 1.0–1.5 eV and represented as much as 20% of the total peak intensity. On the basis of previous investigations of bulk SnS_2, with small percentages of defects, we believe these results are indicative of sites of mixed SnS/SnS_2 material, with photoemission peak splitting due to local surface work function differences. Films of sufficient thickness, with these lower N_S/N_{Sn} ratios, consistently gave a color much darker than the stoichiometric films, consistent with the presence of SnS. While this is a negative result as far as the formation of SnS_2, it does appear that it will be possible to design in substoichiometric sites on the SnS_2 surface by careful control of the fluxes of the metal and dichalcogenide.

In addition to the XPS studies, REELS data were collected (E_p = 200 eV) for each coverage of SnS_2, as a further means of verifying the formation of the desired material and comparison with bulk SnS_2. Figure 4a shows the typical REELS data for a freshly cleaved mica surface. For submonolayer coverages of SnS_2 on mica, Figure 4b shows that the inelastic losses of bulk SnS_2 are beginning to appear (peaks with asterisks in this figure), and that by the time the coverage of SnS_2 on the mica substrate is ca. 2 ML (Figure 4c) the features associated with the principle inelastic energy losses seen for pure bulk SnS_2 (Figure 4d) are fully developed. Studies ongoing in this laboratory[10] have confirmed that when modulated structures are produced involving these metal chalcogenides, these low-energy loss processes can be a sensitive indicator of stoichiometry in the near surface region.[3b,d]

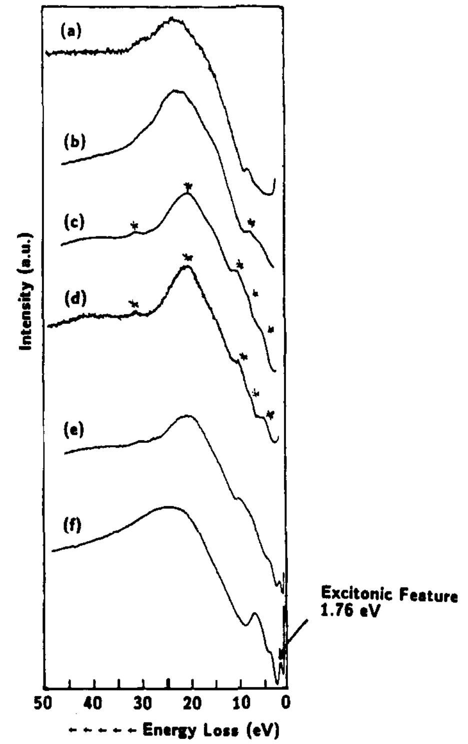

Figure 4. Reflection electron energy loss spectra (REELS) for various coverages of SnS_2 and InPc–Cl, using a primary electron beam energy of 200 eV: (a) freshly cleaved mica, (b) mica with submonolayer SnS_2, (c) multilayer SnS_2 on mica, as for Figure 2c, (d) freshly cleaved bulk SnS_2 to compare with the multilayer SnS_2 in (c), (e) sample in (c) with submonolayer InPc–Cl, (f) sample in (e) with multilayer InPc–Cl. The peaks marked in (b)–(d) are there to indicate the spectral features arising from energy losses in bulk SnS_2.

Optical Properties of SnS_2 Thin Films on Mica. Transmission optical spectra in the visible-wavelength regions were obtained for the MBE grown material and compared with those for bulk SnS_2. Previous optical studies have shown that it is possible to distinguish between the 2H and 4H polytypes of SnS_2 (ABAB versus ABCABC stacking) by careful determination of the bandgap energies for the thin-film materials.[14] Extrapolation of the square root of the product of absorption coefficient and energy, versus optical energy, back to an inflection point near the onset of absorption, allows de-

---

(12) van Hove, J. M.; Pukite, P.; Cohen, P. I. *J. Vac. Sci. Technol.* **1983**, *A1*, 609.

(13) (a) Margaritondo, G.; Rowe, J. E.; Schulter, M.; Kasper, H. *Solid State Commun.* **1977**, *22*, 753. (b) McGovern, I. T.; Williams, R. H.; Parke, A. W. *J. Phys. C: Solid State Phys.* **1979**, *12*, 2689. (c) McMenamin, J. D.; Spicer, W. E. *Phys. Rev. B* **1977**, *16*, 5474.

(14) (a) Grasso, V.; Mondio, G. In *Electronic Structure and Electronic Transitions in Layered Materials*; Grasso, V., Ed.; Reidel: Boston, 1986; pp 260–269. (b) Garg, A. K.; Agnihorti, O. P.; Jain, A. I. K.; Tyagi, R. C. *J. Appl. Phys.* **1976**, *47*, 997.

termination of the band-edge energy, which is ca. 2.29 eV for the indirect gap of the 2H polytype and ca. 2.15 eV for the indirect gap of the 4H polytype. The direct optical transitions are seen at slightly higher energies (2.44 and 2.34 eV, respectively). Our results showed the bandgap energy of the MBE grown SnS_2 thin films to be 2.27 ± 0.10 eV. Films of SnS_2 that were on the order of 100 Å in thickness were nearly transparent, whereas thicker films took on the expected orange–yellow color of bulk SnS_2.

RHEED Studies for InPc–Cl Thin Films Deposited on SnS_2/Mica. Figure 2d shows the RHEED pattern for coverages of InPc–Cl at the monolayer level (or above) on the SnS_2 film characterized in Figure 2c. As reported for CuPc on freshly cleaved MoS_2[5] and InPc–Cl on freshly cleaved bulk SnS_2 and MoS_2,[5,6] the major diffraction lines for the SnS_2 surface lattice, are supplanted by several more closely spaced lines as the coverage of Pc exceeds ca. 0.5 ML. There are five faint lines visible in Figure 2d, including the specular beam at the center of the image. Our measurement of the streak spacing indicates that the Pc surface lattice has a principal component at a spacing of 13.2 ± 0.5 Å. This spacing is consistent with a flat lying ordered array of Pc's, spaced at their van der Waals diameters[5,6] (ca. 13.7 Å).

For Pc films grown on these thin film SnS_2/mica substrates, where the multiple domains noted above were observed, rotation of the sample produced perceptible changes in intensity of the diffraction streaks, and changes in line spacing; however, in general, it was difficult to see a complete loss of the diffraction image of Figure 2d as the sample was rotated. As soon as one diffraction image began to fade, it was replaced by another, with the same streak spacing, as though there are multiple oriented domains of Pc on these SnS_2/mica thin films. Formation of oriented Pc deposits on both of the domain types of SnS_2 we know to be present (noted above) coupled with the poor resolving power of the present phosphor screen technology of these closely spaced diffraction streaks, makes it difficult to unambiguously distinguish the different domains of InPc–Cl forming on the two domains of SnS_2 present on the mica substrate. If the SnS_2 films were appropriately annealed to attenuate the population of these alternate domains (as discussed above), the RHEED data for the monolayer phthalocyanines deposited on these SnS_2 thin films adhered closely to that seen on the bulk SnS_2 and MoS_2 crystals[5a,6] Warming of the SnS_2/mica substrate to a temperature of ca. 300–325 °C for ca. 10 min, causes the original SnS_2 RHEED pattern to be retrieved, suggesting that the Pc layer is desorbed, as would be expected if the Pc layer is held only by weak forces.

As discussed further below, the formation of square lattice domains from flat-lying, 4-fold symmetric molecules such as InPc–Cl, with these square lattices aligned along a principal axis of the SnS_2 substrate, must result in misalignments as these patches coalesce. The fact that reasonable RHEED data are obtained at all from a 4-fold symmetric molecule on a 6-fold symmetric surface is further evidence of the weak interactions between the Pc and the substrate, and the tendency for the first deposited Pc's to template the next to deposit, forming large ordered domains.

Multilayer growth of InPc–Cl films (up to 200–300 Å in thickness) on SnS_2/mica substrates continued to give the high-quality RHEED images seen in Figure 2d. Such patterns could be otained without changing the sample orientation from the position adopted during growth of the first monolayer, and are identical with those diffraction streaks seen for monolayer coverages of InPc–Cl. All of the descriptions of changes in RHEED patterns with rotation of the sample described above, hold for these thicker Pc films. This type of diffraction data was most readily obtained for SnS_2/mica films held at ca. 100 °C during the deposition process and for growth rates of ca. 6 ML/h. Higher growth rates, lower growth temperatures, and/or poorer crystal quality SnS_2 samples (as determined from the RHEED data) did not give the highly oriented multilayer InPc–Cl films.

Optical Characterization of the InPc–Cl SnS_2. Thin Films Formed on Mica. Figure 5a shows the absorbance spectrum of a 10^{-5} M solution of InPc–Cl in chloronaphthalene and the corresponding photocurrent yield spectrum obtained for ca. 0.5 ML of InPc–Cl deposited on a freshly cleaved SnS_2 bulk crystal.[6] On this type of substrate we have shown that the vacuum-deposited InPc–Cl molecules are likely to lie flat on the surface, where the individual molecules pack as close as possible without cofacial overlap. The photocurrent yield spectrum is narrow, has the same vibronic features as the solution spectrum, and is shifted in wavelength by ca. 10–15 nm, consistent with excitation of a molecule missing part of its solvation sphere with a correspondingly altered ground- and excited-state energies.[6] The quantum yield per *absorbed* photon (QYAP) for these InPc–Cl coverages is ca. 50%. We have speculated that such high efficiencies may be due to direct charge injection at defect sites in the SnS_2 surface, which have been previously imaged by scanning tunneling microscopy and which appear to be possible anchor sites for the vacuum deposited Pc.[6] Vacuum deposition above monolayer of coverages of InPc–Cl on the SnS_2 bulk can also produce highly ordered, homogeneous Pc films, as indicated both by RHEED and photocurrent yield spectroscopy[10]. The tendency to form these ordered arrays appears to roughly correlate with the chemistry of atomic defect sites in these surfaces, and is the subject of future investigations.

The absorbance and photocurrent yield spectra of Figure 5a should be contrasted to those of Figure 5b,c which show the absorbance spectra (transmission through the film) of a highly ordered InPc–Cl/SnS_2/mica film (as per the RHEED data of Figure 2f) and a more disordered InPc–Cl/SnS_2/mica film respectively. The disordered film was created on an SnS_2 substrate that did not give clear a RHEED pattern and never showed the sharp diffraction lines of Figure 2f. The absorbance spectrum of the disordered InPc–Cl film is quite similar to those seen for polycrystalline InPc–Cl films, where at least two different crystalline morphologies are seen to coexist.[7,9,15b] Small background absorbances have been removed from both spectra, which arise from light scattering from the mica substrate. The narrowness of the absorbance spectrum of Figure 5b is consistent with the notion that the environment of InPc–Cl is largely homogeneous in this film. The broadening of the absorbance spectrum, normally seen for disordered organic solids, is absent in this material. Some of the highly ordered SnS_2/mica thin films made were unintentionally doped (excess Sn) to make them slightly conductive (sheet resistance ca. 100 kΩ/□), thus allowing photoelectrochemical characterization of the ordered InPc–Cl/SnS_2/mica assemblies (Figure 5d). Although the

---

(15) (a) Kasha, M. In *Spectroscopy of the Excited State*; DiBartole, B., Ed.; Plenum Press: NY, 1976. (b) Dann, A. J.; Hoshi, H.; Maruyama, Y. *J. Appl. Phys.* **1990**, *67*, 1371, 1845. (c) Sims, T.; Pemberton, J. E.; Lee, P.; Armstrong, N. R. *Chem. Mater.* **1989**, *1*, 26. Sims, T. M.S. Thesis, University of Arizona, 1987. (d) Sauer, T.; Caser, W.; Wegner, G. *Mol. Cryst. Liq. Cryst.* **1990**, *183*, 387. (e) Mezza, T. M.; Armstrong, N. R.; Kenney, M. *J. Electroanal. Chem.* **1984**, *176*, 259. (f) Yanagi, H.; Ashida, M.; Elbe, J.; Wörhle, D. *J. Phys. Chem.* **1990**, *94*, 7056.

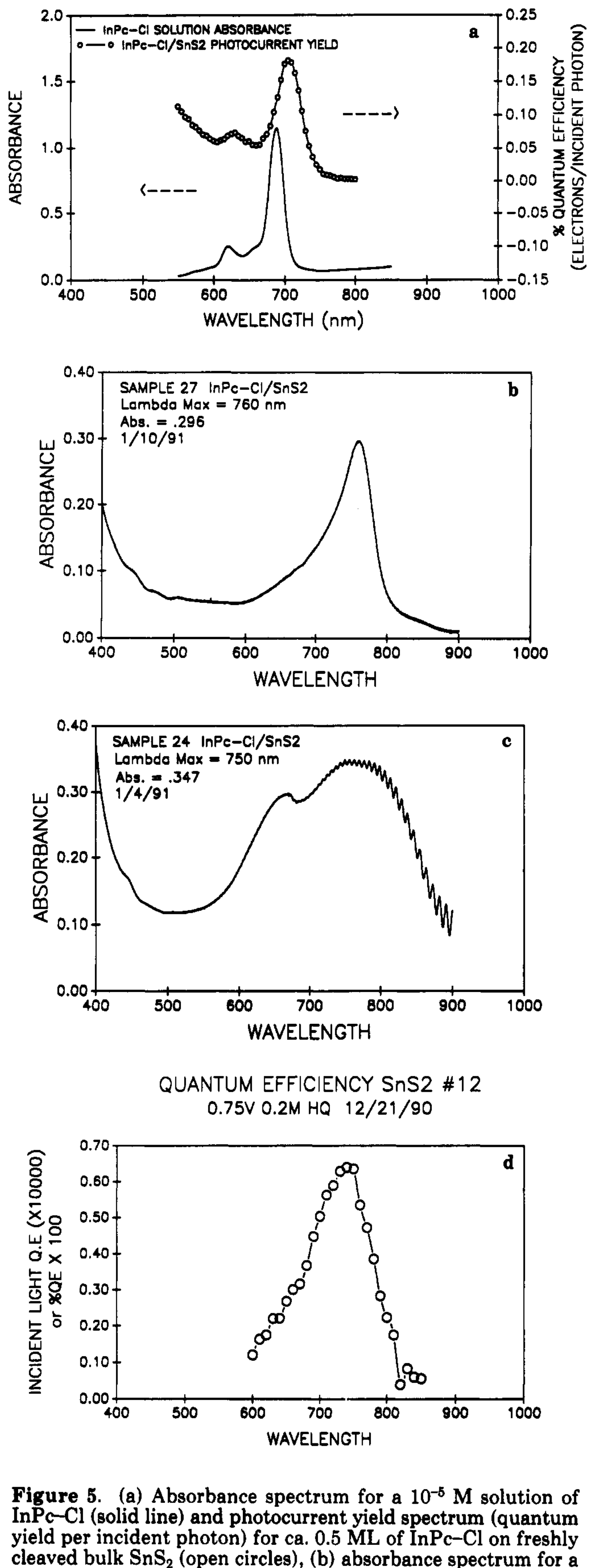

Figure 5. (a) Absorbance spectrum for a 10^{-5} M solution of InPc–Cl (solid line) and photocurrent yield spectrum (quantum yield per incident photon) for ca. 0.5 ML of InPc–Cl on freshly cleaved bulk SnS_2 (open circles), (b) absorbance spectrum for a highly ordered InPc–Cl (as per the RHEED data for Figure 2d), (c) absorbance spectrum for an InPc–Cl film of coverage equivalent to that in (b), except that the RHEED data for this thin film indicated much poorer ordering of the SnS_2 substrate and the InPc–Cl film, (d) photocurrent yield spectrum for a multilayer InPc–Cl/SnS_2 film as in (b).

quantum yields per incident and absorbed photon were poor because of the resistivity of the SnS_2 film, sufficient photocurrent could be harvested to see that these spectra matched the absorbance spectra and that the spectral maxima were the same in both. The photocurrent yield spectra were slightly broader, since the resolution of the monochromator was degraded in order to enhance the photocurrent signal. The phase of Pc giving rise to the absorbance is clearly the only one generating photocurrent. Recent experiments, where InPc–Cl was epitaxially deposited at coverages of 5–10 monolayers on the bulk crystals of SnS_2, gave equivalent photocurrent yield spectra.[6,10]

The perturbation of the ground and excited state energies for adjacent chromophores has been widely described for other types of aromatic systems.[15] Ground-state and excited state energies of the π orbitals are altered by the presence of an adjacent chromophore, spaced at the van der Waals distance, such that both higher and lower energy optical transitions (relative to the monomer in solution) become possible.[15a] The probability of seeing the higher energy, lower energy, or both types of transitions is affected by the orientation of the molecules with respect to each other and by the orientation of their transition dipoles. For smaller aromatic systems, rules have been developed that allow prediction of the probabilities for these transitions. When the trnasition dipoles are oriented parallel to each other, the higher energy transition tends to become favored, and the absorbance spectrum maximum blue shifts. When the transition dipoles are oriented in a head-to-tail alignment, the lower energy transition becomes favored, and the spectra red shift. For chromophores oriented at oblique angles both transitions are allowed, and the spectra split, according to the number of crystallographically inequivalent molecules in the matrix.[15a,d] Sharp, red-shifted (J aggregate) and blue shifted (H aggregate) absorbance maxima have been seen for various cyanine dyes in the past, where the transition dipole orientations were relatively unambiguous.[16] Cofacial, *linear* stacks of phthalocyanines have generally been seen to possess blue-shifted absorbance maxima relative to the monomer in solution.[15b–e] Recent systematic studies of polymeric, cofacial Pc's have been carried out, to demonstrate that these effects are only seen when the proximity of the adjacent Pc rings is near the van der Waals separation distance, ca. 3.2–3.8 Å.[15d] In a recent study involving vacuum-deposited AlPc–F on freshly cleaved KCl crystals, it is apparent that, under the proper growth conditions, only one crystallographic morphology of AlPc–F is formed, consisting of the cofacial, linear Pc stack, which derives from the strong dipolar interactions along the $-Al^{\delta+}-F^{\delta-}-Al^{\delta+}-F^{\delta-}-$ axis.[15b] These Pc layers showed symmetric absorbance peaks and a strong shift in the absorbance maximum to ca. 600 nm, with a fwhm of ca. 60 nm at room temperature suggesting that these molecular crystals also adopt a homogeneous solid-state environment. Staggered or slip stack, cofacial Pc aggregates are presumed to lead to red-shifted spectra, although to our knowledge there has not been a unique correlation between the absorbance spectrum and the single crystal structures of the Pc responsible for this red-shift. Most thin films of Pc's that show the red shift in the absorbance spectrum also consist of more than one phase of the material.[15c] It will be of interest in future studies to determine the extent to which the shoulder at ca. 680 nm in the spectrum of Figure 5b represents a transition to a part of

---

(16) (a) Czikkely, V.; Försterling, H. D.; Kuhn, H. *Chem. Phys. Lett.* 1970, *6*, 11. (b) Büchner, H.; Kuhn, H. *Chem. Phys. Lett.* **1970**, *6*, 183.

the exciton manifold of the Pc aggregate or the onset of another phase of InPc–Cl, which grows in relation to the disorder in the system.[15a]

Differences exist in the absorptivities of InPc–Cl that were deposited in an ordered fashion, versus the more polycrystalline material. The absolute coverage of InPc–Cl was determined for the samples represented in Figures 5b,c, by dissolving these Pc films into known volumes of pyridine and using the solution absorbance spectra to quantitate the absolute number of moles per unit area. For the highly ordered InPc–Cl film in Figure 5b, $A_{760\mathrm{nm}}$ = 0.282 and $\Gamma_{\mathrm{InPc-Cl}}$ = ca. 4.5×10^{-9} mol/cm^2, whereas for the polycrystalline InPc–Cl film in Figure 5c, $A_{760\mathrm{nm}}$ = 0.230 and $\Gamma_{\mathrm{InPc-Cl}}$ = ca. 1.3×10^{-8} mol/cm^2. Determining the thickness of each film is problematic, since it involves assumptions regarding the orientation of the Pc molecules in the thin film with respect to the substrate. For the flat-lying InPc–Cl in the highly ordered material in Figure 5b, we estimate $\beta = 3.9 \times 10^5$ cm^{-1}. The ratio of absorbances for these two thin films, normalized to surface coverage, is ca. 3.5. Further determinations of this difference in absorptivity, at lower surface coverages are in progress, and indicate that larger values of β are determined as the coverage of Pc is reduced.

These linear optical properties in the visible-wavelength region may prove to be an extremely sensitive indicator of ordering in a Pc layer. Interestingly, recent studies of vanadylnaphthalocyanines deposited onto the KCl [001] surface gave excellent high-resolution electron microscopy and electron diffraction images, suggesting ordering, and yet still produced absorbance spectra suggestive of a somewhat polycrystalline thin film.[15f] No attempts were made to measure relative absorbance values in the ordered versus disordered materials.

Models for van der Waals Epitaxy of the SnS_2/Mica and InPc–Cl/SnS_2. The description of the growth of thin films like SnS_2 on mica as arising strictly from van der Waals interactions with the substrate[3] may be somewhat simplistic for the first monolayer, since their is some clear directionality given to the SnS_2 nuclei by the mica substrate, and weak interactions alone would not be expected for such a highly defective structure as a freshly cleaved mica surface. If, however, epitaxy is defined as that process that leads to an overlayer with a structure somewhat coincident with the substrate, and low interfacial energy relative to the random arrangement,[1] then the deposition of these metal dichalcogenides clearly represnts a class of heteroepitaxy. Subtle channels present in the mica surface, which have been documented previously,[3b] may act to "guide" the formation and nucleation of the initial unit cells for the metal sulfide. Because of the weak interaction between adjacent sulfide layers, this "guiding" process probably need only extend to the first full monolayer of SnS_2 formed, before natural crystallization processes take over, i.e., lattice strain is quickly relieved. The exact mechanism for the formation of the initial SnS_2 nuclei, however, remains a subject requiring additional study, especially with regard to the formation of the additional oriented domains of SnS_2, the reason for their rotation from the major domains by ca. 30°, and the attenuation of these domains during annealing.

Temperatures above ca. 325 °C and sulfur partial pressures above 1×10^{-9} Torr, with Sn beam fluxes of less than 10 Å/min seem to be necessary to ensure deposition of stoichiometric SnS_2. Sulfur pressures below those levels and/or substrate temperatures below 325 °C appear to produce sulfur-deficient sulfides, with poorer quality RHEED images. The optimal processing conditions for these materials are still not known, and it may be that faster growth rates and lower processing temperatures will be possible. Comparison with other semiconductor and metal systems created by using MBE technologies shows that thin films of these layered materials may require less stringent processing conditions, especially with regard to the vacuum requirements necessary to produce stoichiometric and impurity-free films. The low sticking coefficients of most small molecules on the dichalcogenide surface undoubtedly plays a role in helping to keep these materials clean as they are growing.[11,17] It is clear that formation of high quality SnS_2 thin films is possible, transparent to a large fraction of the visible-wavelength region, which provide an excellent substrate for the single-crystal deposition of vacuum-compatible organics. Extrapolation of this finding to additional optically interesting materials is underway.

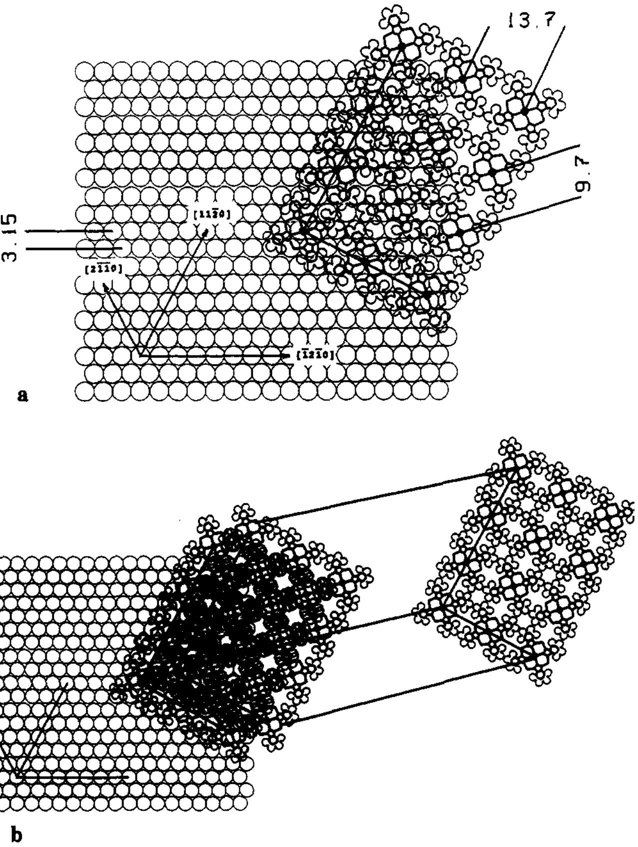

Figure 6. Schematic of a possible packing pattern for InPc–Cl on the SnS_2 surface, at (a) monolayer coverage and (b) multilayer coverages, consistent with the single-crystal diffraction studies of related Pc's[22] and the optical properties of the InPc–Cl/SnS_2/mica thin films.

A proposed model of the InPc–Cl overlayer on the freshly deposited SnS_2 surface is shown in Figure 6a. This orientation of the Pc appears to allow for the 4-fold symmetric molecule to find an orientation on the hexagonal closest packed sulfide surface, without the need for forming a commensurate structure, which results in an oriented overlayer, as indicated by RHEED. The orientation and spacing of the Pc molecules in this figure are similar to those suggested from previous studies of metalated phthalocyanines, which had been shown to form epitaxial monolayers on a Cu(100) surface.[18a] On that substrate metal, the correspondence of the surface metal atoms and the bridging nitrogens in the Pc formed a nearly com-

---

[17] Griffiths, C. H.; Walker, M. S.; Goldstein, P. *Mol. Cryst. Liq. Cryst.* **1970**, *33*, 149.

mensurate structure, such that the Pc rings could closest pack at the van der Waals distances. Subsequent scanning tunneling microscopic images of such a surface clearly showed the Pc rings arranged in that fashion, forming a square lattice, with the benzenoid rings touching.[18b] Our spectroscopic and photoelectrochemical studies (and as shown above) have confirmed that, at Pc coverages well below monolayer, there is a small perturbation of the excited-state energies of these closely space chromophores.[6]

The array shown in Figure 6 (inspired by these previous studies) would provide the necessary 13.7-Å spacing along the SnS_2 principle axis, would produce the same RHEED pattern every 60° and would provide a larger RHEED spacing (by $\sin(45°) \approx \sqrt{2}$) by rotating the crystal by 45° from the principle axis. The demonstration of a true square lattice would be made more straightforward using a substrate with 4-fold symmetry, which also formed some type of commensurate structure with the Pc overlayer[5b] and which would allow for only one orientation of the flat-lying Pc lattice. The RHEED data shown here and obtained on freshly, cleaved bulk SnS_2 with InPc–Cl, suggest that large square lattice domains of InPc–Cl are created, aligned along a principal axis of SnS_2, so that rotation of the sample brings one of the principle axes of these overlayers into a favorable position for the formation of the RHEED streaks seen in Figure 2d, every 60°. The wider spaced diffraction streaks corresponding to the 45° rotation of the square lattice are occasionally at our detection limits, accompanying the onset of the major diffraction streaks seen in Figure 2d.

Our previous STM studies have shown the presence of oriented InPc–Cl molecules on MoS_2 surfaces, where the Pc molecules appeared to be anchored at atomic defect sites in the MoS_2 surface, with the halide part of the In–Cl bond protruding into the defect site.[6] Interestingly, these Pc's all had adopted an orientation consistent with the RHEED images for this same surface, and consistent with the RHEED images seen here for comparable coverages of InPc–Cl on *both* SnS_2 and MoS_2[5,6]—that is the orientation suggested in Figure 6. There are problems imaging some forms of SnS_2 with the STM, including the MBE-grown material here, because of its tendency to "etch" during the imaging process,[20] so no comparable images for that material have yet been obtained. Atomic force microscopy is currently under exploration to determine whether acceptable images can be obtained by this approach.

Although no single crystal studies of the InPc–Cl system exist (to our knowledge), there have been several such studies done for one or more phases of related materials, including GaPc–Cl and AlPc–Cl,[21] TiOPc,[22] and VOPc.[23] The GaPc–Cl structure, published by Wynne,[21] is likely to be the closest to at least one of the possible forms that InPc–Cl might adopt in the solid state. In this study it was demonstrated that the Pc ring is largely planar, with the dimensions suggested above, but that the metal atom lies above the plane of the ring by ca. 0.44 Å. By looking at the same distance for the AlPc–Cl system (the Al atom lies above the plane of the ring by ca. 0.41 Å), we can expect that the In atom will lie above the plane of the Pc ring in InPc–Cl by almost 0.5 Å. Such distances for distortion of the molecule have been documented for indium porphyrin systems.[24] This distorted, square pyramidal geometry might provide a topology to the InPc–Cl molecule that would allow it to directly interact with atomic defect sites in the SnS_2 surface, orienting the Pc face down on the surface, with the halide protruding into the defect site (again by inference to other structures of Pc's and porphyrins, we expect the halide to be situated nearly 3 Å from the plane of the Pc ring, thus allowing interaction of the anion with the cations in these surface defects[19]). It should be pointed out, however, that we[6] and Hara and co-workers,[5] have been able to achieve comparable crystalline monolayers of CuPc and MoS_2 (as indicated by RHEED), and this is a nearly flat molecule, with no axial group attached to the metal.

It appears likely that the square-symmetry molecules come to rest during the deposition process at edge sites on the chalcogenide surface, which accommodate such molecular shapes, and act to "template" a monolayer of flat lying, noninteracting Pc's. These metal dichalcogenides are also known to intercalate smaller aromatic molecules,[25] and there exists the possibility that some partial intercalation of the initially deposited Pc helps to set the arrangement for the subsequently deposited materials. Angle-resolved XPS, which should be sensitive to intercalation of the Pc completely under the SnS_2 surface, does not indicate that such processes are occurring beyond the first monolayer of Pc. It seems unlikely that an intercalated equivalent monolayer of InPc–Cl would be capable of supporting the epitaxial deposition of subsequent Pc layers. Further tests of this assumption with a wider range of Pc's and with other vacuum-compatible chromophores, are underway.

Once the first monolayer of Pc is complete, growth of the second layer could be commensurate with the first layer, or the molecules may adopt a "tilted" or upright orientation with respect to the surface. Higher packing densities are certainly possible if the upright orientation is chosen. This packing of Pc molecules will undoubtedly lead to changes in the RHEED patterns that were not seen for our deposition experiments. Since the RHEED experiment is most sensitive to the upper 1–2 molecular layers of material, the fact that no changes in the RHEED patterns were seen for Pc coverages of up to 50 ML suggests that no change in Pc orientation with respect to the surface has occurred.[12] Again, the single-crystal diffraction studies of Wynne for GaPc–Cl,[21] and similar studies of related Pc's suggest a packing pattern that may be consistent with the observed electron diffraction data. GaPc–Cl is able to adopt a packing pattern in which layers of adjacent Pc's all possess the halide pointing in one direction, and the next layer on top simply shifts each ring over by ca. one-half a molecular diameter, and positions the halide down. This kind of ABAB packing does not change the distance between adjacent Pc's within each layer and accommodates the distorted geometry caused by the out-of-plane metal and halide centers.

Figure 6b indicates a possible packing pattern for the second layer of Pc over the first one indicated in Figure 6a, consistent with this type of packing geometry. Each Pc ring has been spaced over by ca. one-half a molecular

---

(18) Hiller, W.; Strahle, J.; Kobel, W.; Hanack, M. *Z. Kristalogr.* **1982**, *33*, 173.

(19) Stickney, J. S.; Rosasco, S. R.; Solomun, T.; Hubbard, A. T.; Parkinson, B. A. *Surf. Sci.* **1984**, *136*, 15.

(20) (a) Buchholz, J. C.; Somorjai, G. A. *J. Chem. Phys.* **1977**, *66*, 573. (b) Lippel, P. H.; Wilson, R. J.; Miller, M. D.; Wöll, Ch.; Chiang, S. *Phys. Rev. Lett.* **1989**, *62*, 171.

(21) (a) Parkinson, B. A. *J. Am. Chem. Soc.* **1990**, *112*, 7498. (b) Suna, A.; Parkinson, B. A., to be published.

(22) (a) Wynne, K. J. *Inorg. Chem.* **1984**, *23*, 4658. (b) Hiller, W.; Strähle, J.; Kobel, W.; Hanack, M. *Z. Kristallogr.* **1982**, *159*, 173.

(23) Ball, R. G.; Lee, K. M.; Marshall, A. G.; Trotter, J. *Inorg. Chem.* **1980**, *19*, 1463.

(24) Kasztelan, S. *Langmuir* **1990**, *6*, 590.

(25) O'Hare, D.; Jaegermann, W.; Williamson, D. L.; Ohuchi, F. S.; Parkinson, B. A., *Inorg. Chem.* **1988**, *27*, 1537.

diameter. This orientation allows for the metal halide bonds in adjacent Pc layers to align in an opposed fashion. This model does not address the orientation of the Pc's in the first layer (halide up or halide down), and does not rule out the possibility that the first layer of Pc will adopt a slightly different attitude with respect to the surface plane than subsequent deposited layers. Present RHEED technologies do not have sufficient resolution in measuring the spacing between diffraction streaks for these large molecules to discriminate such subtle effects, however, studies in progress promise that additional structural information can be obtained by refinements in the technology.

Previous studies of vanadylphthalocyanine have tried to demonstrate the correlation between stacking of the adjacent Pc's and the visible absorbance spectra of thin films of such materials.[23] It has been suggested that the slipped stacking pattern like that of Figure 6b will lead to a red-shifted absorbance maximum. To our knowledge however, there have been no studies of true single-crystal thin film Pc's where a strict comparison of the absorbance spectrum and the crystallographic orientation has been done.

The optical data of Figure 5 demonstrate that the Pc multilayer formed must be nearly homogeneous, as indicated by the narrowness of the major abosrbance peak. The origin of the shoulder on the blue side of this absorbance peak is not clear, but since its intensity with respect to the major peak is constant over a wide range of Pc film thicknesses, it suggests that it arises from the same type of vibronic coupling seen in the solution monomer absorbance spectra.[13-15] It is clear that a complete structural analysis of such thin Pc layers will be necessary in order to fully assign these spectral features.

It appears possible now, however, to grow organic thin films, with thicknesses necessary for reasonable linear and nonlinear optical characterization, by the MBE approach.[10] The combination of metal dichalcogenide formation on transparent substrates, and the ordered growth of the subsequent organic layer, may allow for the formation of organic layers with high optical density, with narrow excitonic bands in a desirable wavelength range, which lead to interesting new studies in the areas of photoconduction, optical switching, and optical data storage.

Acknowledgment. We gratefully acknowledge support for this research from the National Science Foundation and the Materials characterization Program—State of Arizona. We are also grateful to Bruce Parkinson and Fumio Ohuchi for the samples of bulk SnS_2 and for several helpful discussions throughout the course of these studies.

Registry No. InPc–Cl, 19631-19-7; SnS_2, 1315-01-1.

Properties of Ion-Exchange Membranes Combined Anisotropically with Conducting Polymers. 2. Relationship of Electrical Potential Generation to Preparation Conditions of Composite Membranes

Toshikatsu Sata

Research and Development Division, Tokuyama Soda Co., Ltd., Mikage-cho 1-1, Tokuyama City, Yamaguchi Prefecture, 745, Japan

Received February 14, 1991. Revised Manuscript Received July 2, 1991

Preparation and properties of cation-exchange membranes with which polypyrrole had been combined anisotropically were studied in detail. When one side of a cation-exchange membrane in the ferric ion form contacted an aqueous pyrrole solution for a given period, pyrrole polymerized easily and quickly and formed a polypyrrole layer in the membrane matrix beginning from the membrane surface. The polypyrrole layer was so tight that pyrrole molecules could not permeate it in 50 h of exposure. X-ray microanalysis of a cross section of the membrane revealed its anisotropic structure. During this oxidative polymerization of pyrrole, more than 90% of the ferric ions in the membrane phase were reduced to ferrous ions. On the surface of the membrane opposite the polypyrrole layer was a cation-exchange membrane layer that contained ferric ions, while most of the membrane contained ferrous ions. When this composite membrane was held tightly between two platinum plates, a electrical potential was observed because of Fe^{2+}–Fe^{3+} redox reactions. To confirm this further, a ferric ion form of a cation-exchange membrane and a cation-exchange membrane in which polypyrrole had been impregnated from both surfaces were clamped together tightly between two platinum plates and placed into pure water to hydrate the membranes. A higher electrical potential was observed when compared with the composite membrane.

Introduction

Polypyrrole, polyaniline, other conducting polymers, and their analogues have been widely studied in the field of pure and applied materials chemistry.[1-5] Examples of their possible applications include batteries,[6-11] electrochromic displays,[12-14] solid electrolytic capacitors,[15] etc. I

---

(1) Diaz, A. F.; Kanazawa, K. K.; Gardini, G. P. *J. Chem. Soc., Chem. Commun.* **1979**, *635*, 854.

(2) Pratesi, P. *Gazz. Chim. Ital.* **1937**, *67*, 183.

(3) Khulbe, K. C.; Mann, R. S. *J. Polym. Sci., Polym. Chem. Ed.* **1982**, *20*, 1089.

(4) Angeli, A.; Lutri, C. *Gazz. Chim. Ital.* **1920**, *50*, 128.

(5) Diaz, A. F.; Gastillo, J. I.; Kanazawa, K. K.; Logan, J. A.; Salmon, M.; Fajardo, O. J. *J. Electroanal. Chem.* **1981**, *133*, 233.

(6) Mohammadi, A.; Inganas, O.; Lundstrom, I. *J. Elecrochem. Soc.* **1986**, *133*, 947.

(7) Mermilliod, N.; Tanguy, J.; Petiot, F. *J. Electrochem. Soc.* **1986**, *133*, 1073.

(8) Diaz, A. F.; Logan, J. A. *J. Electroanal. Chem. Interfacial Electrochem.* **1980**, *111*, 111.

(9) MacInnes, D., Jr.; Druy, M. A.; Nigery, R. J.; Nairns, D. P.; MacDiarmid, A. G.; Heeger, A. J. *J. Chem. Soc., Chem. Commun.* **1981**, 317.

(10) Diaz, A. F.; Castillo, J. L.; Logan, J. A.; Lee, W. Y. *J. Electroanal. Chem. Interfacial Electrochem.* **1981**, *129*, 115.

0897-4756/91/2803-0838$02.50/0